Review of Scientific Instruments

The response function of Fujifilm BAS-TR imaging plates to laser-accelerated titanium ions

Cite as: Rev. Sci. Instrum. **90**, 083302 (2019); https://doi.org/10.1063/1.5109783
Submitted: 12 May 2019 . Accepted: 12 July 2019 . Published Online: 08 August 2019

J. Strehlow, P. Forestier-Colleoni, C. McGuffey, M. Bailly-Grandvaux, T. S. Daykin, E. McCary, J. Peebles, G. Revet, S. Zhang, T. Ditmire, M. Donovan, G. Dyer, J. Fuchs, E. W. Gaul, D. P. Higginson, G. E. Kemp, M. Martinez, H. S. McLean, M. Spinks, H. Sawada, and F. N. Beg

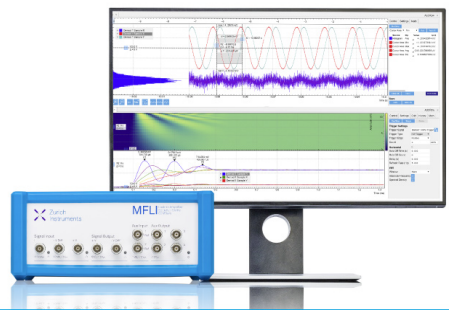

Review of Scientific Instruments ARTICLE scitation.org/journal/rsi

The response function of Fujifilm BAS-TR imaging plates to laser-accelerated titanium ions

Cite as: Rev. Sci. Instrum. 90, 083302 (2019); doi: 10.1063/1.5109783
Submitted: 12 May 2019 • Accepted: 12 July 2019 •
Published Online: 8 August 2019

J. Strehlow,[1] P. Forestier-Colleoni,[1] C. McGuffey,[1] M. Bailly-Grandvaux,[1] T. S. Daykin,[2] E. McCary,[3] J. Peebles,[4] G. Revet,[5] S. Zhang,[1] T. Ditmire,[3] M. Donovan,[3] G. Dyer,[6] J. Fuchs,[5] E. W. Gaul,[3] D. P. Higginson,[7] G. E. Kemp,[7] M. Martinez,[3] H. S. McLean,[7] M. Spinks,[3] H. Sawada,[2] and F. N. Beg[1,a)]

AFFILIATIONS

[1]Department of Mechanical and Aerospace Engineering, University of California–San Diego, La Jolla, California 92093, USA
[2]Department of Physics, University of Nevada, Reno, Nevada 89557, USA
[3]Center for High Energy Density Science, University of Texas, Austin, Texas 78712, USA
[4]Laboratory for Laser Energetics, Rochester, New York 14623, USA
[5]LULI, Ecole Polytechnique, Route de Saclay, 91128 Palaiseau, France
[6]SLAC National Accelerator Laboratory, Menlo Park, California 94025, USA
[7]Lawrence Livermore National Laboratory, Livermore, California 94550, USA

[a)]**Electronic mail:** fbeg@ucsd.edu

ABSTRACT

Calibrated diagnostics for energetic particle detection allow for the systematic study of charged particle sources. The Fujifilm BAS-TR imaging plate (IP) is a reusable phosphorescent detector for radiation applications such as x-ray and particle beam detection. The BAS-TR IP has been absolutely calibrated to many low-Z (low proton number) ions, and extending these calibrations to the mid-Z regime is beneficial for the study of laser-driven ion sources. The Texas Petawatt Laser was used to generate energetic ions from a 100 nm titanium foil, and charge states Ti^{10+} through Ti^{12+}, ranging from 6 to 27 MeV, were analyzed for calibration. A plastic detector of CR-39 with evenly placed slots was mounted in front of the IP to count the number of ions that correspond with the IP levels of photo-stimulated luminescence (PSL). A response curve was fitted to the data, yielding a model of the PSL signal vs ion energy. Comparisons to other published response curves are also presented, illustrating the trend of PSL/nucleon decreasing with increasing ion mass.

I. INTRODUCTION

Imaging plate (IP) detectors have a multitude of advantages over other detectors for use in laser-plasma experiments. Unlike a CCD, the IP is not affected by the electromagnetic pulse often produced by laser-plasma interactions.[1] Their high dynamic range, on the order of 10^5, enables them to detect a wide range of particle species and energies.[2,3] Additionally, they are erasable, unlike other single-use dose deposition detectors, such as CR-39 and radiochromic film (RCF).[3] Although there exist robust IP calibrations for x-rays, electrons, and several low-Z (low proton number) ions,[1,3–10] no imaging plate calibrations have been published for any ions heavier than carbon. The BAS-TR IP is ideal for the detection of heavier ions since, unlike other IP types, it lacks a protective layer of Mylar.[3,8]

The established IP calibrations have allowed for more accurate characterization of plasma physics phenomena, with applications such as nuclear fusion,[11] x-ray radiography,[4] and particle acceleration.[3,9] To advance the study of laser-ion acceleration, response functions of imaging plates to mid-Z ions are beneficial in order to compare the theoretical energy spectra of various acceleration models. Titanium was specifically chosen in order to advance the understanding of mechanisms of laser-ion acceleration from ultrathin titanium targets. In this ultrathin, mid-Z regime, there are multiple possible competing mechanisms, not limited to, target normal

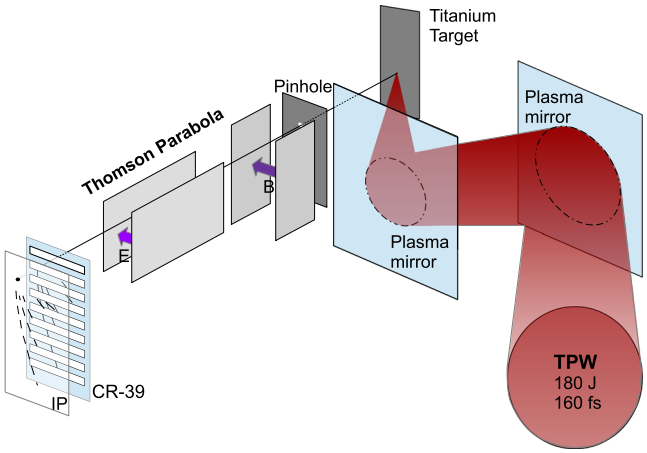

FIG. 1. Diagram of the experimental setup corresponding to the front Thomson parabola. Double plasma mirrors enhanced the laser contrast by 10^4. Figure not to scale.

sheath,[12] radiation pressure,[13] and relativistic induced transparency acceleration.[14]

The Fujifilm BAS-TR imaging plate was originally developed for high resolution tritium detection. The 50 μm active layer is composed of $BaFBr_{0.85}I_{0.15}:Eu^{2+}$, with a density of 2.85 g/cm^3, which is supported by a 250 μm polymer layer. These layers are followed by a 160 μm magnetic layer for attachment to the IP scanner.[8] When incident radiation deposits energy into the active layer, the detector stores the energy as phosphorescence, exponentially decaying to 50% of its maximum intensity over 3 h.[9] After a standardized reference time, typically 30 min in the literature, the IP is then scanned, yielding the standardized signal PSL_{30}. If the IP is not scanned at the reference time, the PSL signal can be adjusted to PSL_{30} via an empirical exponential model for the fade time of the active layer.[3,9] Prior to reuse, the IP is erased with a bright white light source for tens of minutes.[3]

In this paper, the authors summarize their procedure to calibrate the BAS-TR IP to energetic titanium ions. The limitations of the calibration are discussed, along with the implementation of theoretical models of the IP response. Comparisons to other published response functions yield an empirical model that estimates the IP response for any ion of a given atomic mass.

II. EXPERIMENTAL METHODOLOGY

The Texas Petawatt Laser created the laser-driven ion source, in conjunction with a campaign on investigating titanium acceleration from ultrathin titanium targets. Upstream from the target, double plasma mirrors enhanced the laser contrast from 10^{-9} to 10^{-13} beyond 100 ps. Without this high laser contrast, the prepulse from the laser would destroy the ultrathin 100 nm target. The 1 μm wavelength laser directed 50 J on the target, with a FWHM intensity of 5×10^{20} W/cm^2. Two Thomson parabolas (TPs),[15] one along target normal and one 11° off-axis, were employed to study rear acceleration mechanisms, and a third measured the front acceleration for this calibration of the imaging plates with CR-39. IP detectors are often calibrated for ions with CR-39 track detectors.[3,5,7,9] When incident on this plastic, energetic ions create a track of broken polymer chains within the bulk. The particle tracks can be etched to tens of microns with a strong base and then viewed under an optical microscope. Particle track size is a function of etching time, etching solution concentration, and temperature. It is important not to overetch because the tracks can overlap and become difficult to distinguish.[16]

To measure the deposited dose of titanium ions on the IP, a CR-39 track detector with periodic slots was superimposed upon the IP. The detector has slots and spacings of each 1 mm, allowing for a direct comparison of the deposited dose to the PSL signal from the shadow of the CR-39 (Fig. 1).

The front TP shown in Fig. 1 was used for the calibration shot. After the shot, the CR-39 was etched in 6.25M NaOH solution for 3 h at 75° C, to get a titanium track diameter of ~17 μm, as observed under an optical microscope at 40× magnification (Fig. 2).

III. DETERMINING THE IP RESPONSE TO TITANIUM IONS

Each IP was scanned approximately 30 min after each shot, with a General Electric Typhoon FLA 7000 IP scanner. The scanner settings are as follows: 25 μm resolution, latitude 5, sensitivity 4000, and PMT 500 V. After scanning, the calibration shot IP was analyzed to determine the ion species and their corresponding energy spectra. A linear interpolation was employed to find the average PSL value best corresponding to each slot of CR-39, and this value was matched with the ion number per solid angle. The ions were counted from microscope images following the etching procedure.

The Thomson parabola spectrometer separated the protons, carbons, and titanium ions, creating parabolic traces on the CR-39

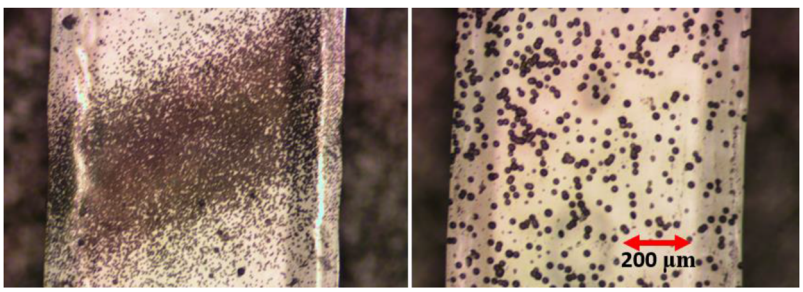

FIG. 2. Comparison of proton (left) and titanium (right) ion tracks after etching.

TABLE I. Titanium calibration curve fit parameters. The fit is of the form $PSL_{30}/ion = aE^b$, where E is in MeV.

Species	a	b	R^2
Ti^{10+}	0.2240	0.2315	0.9815
Ti^{11+}	0.2821	0.1459	0.8488
Ti^{12+}	0.2376	0.2101	0.9999
Combined species	0.2317	0.2174	0.9722

and IP stack (Fig. 1). The titanium ions were counted under a microscope and corresponded to a PSL value that was calculated from the average PSL on each side of the CR-39 detector. The resulting calibration from this analysis, conducted with Ti^{10+}, Ti^{11+}, and Ti^{12+} (Table I, Fig. 3) displays a charge-independent relationship of PSL_{30}/#Ti-ions vs incident ion energy. Although stopping power is proportional to the square of the charge species, IP response is not charge dependent as long as the same amount of energy is deposited in the 50 μm active layer. This charge independence is expected to hold for all other ionization states of titanium, which is consistent with the BAS-TR IP calibration for energetic carbon ions.[3] Because conducting the calibration requires averaging absolute dose and PSL counts over a fixed area, a small uncertainty arises in the PSL response data. Additionally, some of the etched ion tracks largely overlapped, resulting in a small uncertainty in the deposited dose. This same calibration procedure was conducted for 53 MeV carbon ions, deposited on one slot of CR-39, to support the published BAS-TR IP calibration for carbon ions.[3] There is good agreement between the published IP response function for carbon and the datum determined from this analysis, as represented in Fig. 7.

The titanium data demonstrate a power law relationship that is limited to extrapolation for titanium ions between 4.8 and 161 MeV. Figure 4 illustrates simulations conducted using Stopping and Range

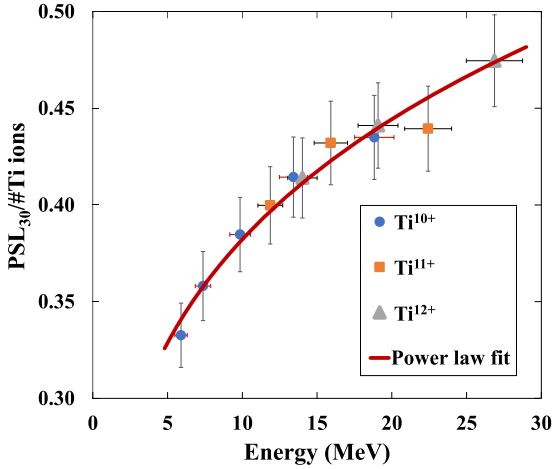

FIG. 3. IP response to energetic titanium ions. The data are best fit by the power model $PSL_{30}/ion = aE^b$, where E is in MeV. Plotted below is the fit with all three charge species, demonstrating charge independence. The corresponding fit parameters and coefficients of determination are shown in Table I.

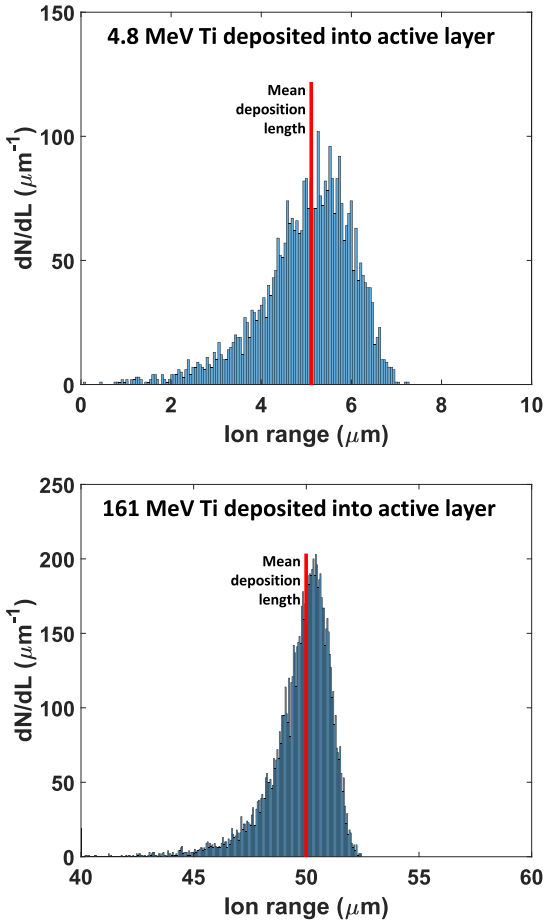

FIG. 4. Simulations deposited 10 000 monoenergetic titanium ions into the BAS-TR IP, indicating the limitations of the calibration curve. In the top figure, 4.8 MeV titanium ions are deposited in the active layer. At this energy, the PSL signal becomes highly statistical because the range is smaller than the 5 μm grain size.[3] The lower figure illustrates the calibration's high bound of 161 MeV, as at this energy, the ions fully penetrate the 50 μm active layer.

of Ions in Matter (SRIM),[17] which indicates that 4.8 MeV titanium ions have an average penetration depth of 4.97 μm in the active layer. This depth is just below the grain size of 5 μm. With a penetration depth less than the grain size, the imaging plate response becomes highly statistical.[3] Additionally, SRIM calculations determined that titanium ions exceeding 161 MeV have a high probability of penetrating the 50 μm active layer. A calibrated spectrum, plotted within these limits, is shown in Fig. 5.

This empirical response function allows for the calculation of the IP sensitivity to titanium ions, in units of PSL/MeV. Hidding's model of IP response to radiation[18] assumes that the response $R(E)$ is proportional to the energy deposited, as

$$R(E) = \alpha E_{dep}(E), \quad (1)$$

where α is the sensitivity in PSL per units of energy deposited. This is valid at high energies for low-Z ions when the stopping power

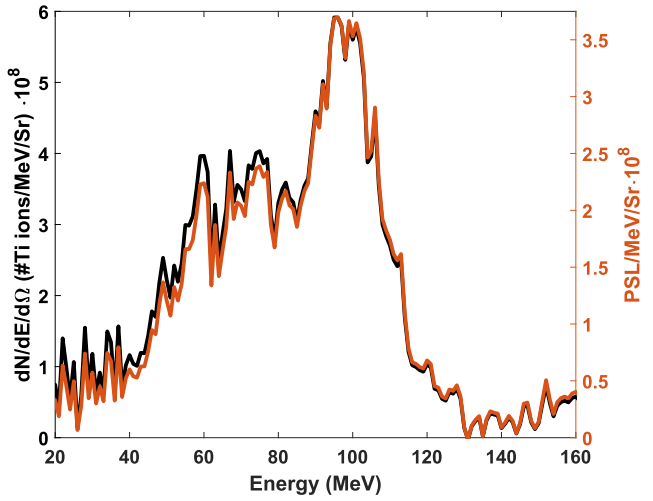

FIG. 5. Energy spectrum of Ti^{12+} accelerated from the rear side of a 60 nm titanium foil. The black curve displays the applied calibration, and the red curve shows the uncalibrated spectrum in units of PSL.

is approximately constant. However, a more accurate model (Bonnet's model) accounts for variation in stopping power, as well as the absorption of the PSL photons inside the active layer of the IP,

$$R(E) = \alpha \int_0^T \frac{dE}{dx} exp(-x/L)dx, \quad (2)$$

where T is the thickness of the active layer and L is the absorption length of the PSL photons.[7] The simulation package SRIM[17] produced simulated stopping power values within the IP active layer. These tabulated data cover the full range of energies valid for the IP response function.

In the energy regime of this calibration (4.8–161 MeV), the titanium ions do not penetrate the active layer, yielding a sensitivity that depends strongly upon the stopping power. Hence, Hidding's stopping-power independent model is a very loose approximation of the IP response, with a sensitivity $\alpha = 0.0227 \pm 0.0174$ PSL/MeV. Implementing Bonnet's model reveals far greater precision, yielding $\alpha = 0.0037 \pm 0.0008$ PSL/MeV. The uncertainty was determined from the standard deviation in averaging the tabulated values of α.

According to Bonnet's model, the IP response to protons is twice as sensitive as that to titanium.[7,8] For protons, Hidding's and Bonnet's models produce sensitivities within the same order of magnitude. However, this is not the case for heavier ions such as titanium, as Bethe's stopping power formula is proportional to the square of the charge state.[19] The large disagreement between Hidding's and Bonnet's models is reconciled by the increased role of stopping power for heavier ions. Bonnet's studies also indicate an IP quenching effect dependent upon stopping power.[6] This quenching effect agrees with the calculations presented here. Particles with greater stopping power have a lower IP sensitivity, similar to the response of an organic scintillator.[20]

These models are visualized in Fig. 6, implying that Hidding's model cannot be soundly applied to energetic ions in the mid-Z regime. Bonnet's model does more closely approximate the empirical fit but has a peak that is not predicted by the SRIM calculations

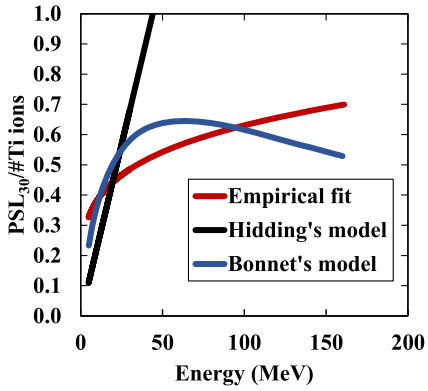

FIG. 6. Hidding's and Bonnet's models compared against the empirical IP calibration curve fitted in Fig. 3. Hidding's linear fit model proves to be a poor representation, whereas Bonnet's model demonstrates a more accurate trend. Note that Bonnet's model predicts a peak in the IP response due to the absorption of PSL photons within the active layer.

of stopping power. This peak originates instead from Bonnet's prediction that PSL photons generated deep within the active layer are absorbed before they can escape. However, this model is still a weak fit to the data ($R^2 = 0.5348$), while the empirical model appears to be a better representation of the IP response ($R^2 = 0.9722$). Studies of higher energy titanium ions are warranted to determine the energy where the titanium response function begins a decreasing trend.

IV. COMPARISON OF ESTABLISHED IP CALIBRATIONS

Once the ions fully penetrate the active layer, the depth of the Bragg peak will exceed the thickness of the active layer. Hence, the ions will deposit exponentially less energy into the active layer as

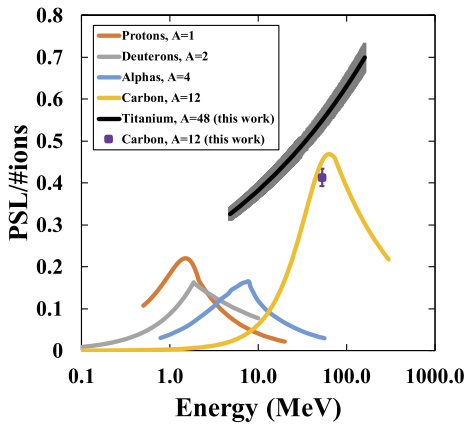

FIG. 7. BAS-TR IP response curves for ions of varying atomic mass A. Each low-Z calibration shows the peak representing the ion fully penetrating the active layer.[3,5,6,9] The titanium calibration, shown with error bands in its full theoretical range of validity, does not show this peak because no ions were accelerated into the necessary energy domain (>161 MeV). An additional carbon calibration point from this experiment is included.

TABLE II. Fit parameters for the IP response vs atomic mass unit A. The fit is of the form $PSL_{30}/ion/amu = aA^b$.

Species	a	b	R^2
Previous calibrations[3,5,6,9]	0.1599	−0.6769	0.8075
Previous calibrations + this work	0.1531	−0.6244	0.9049

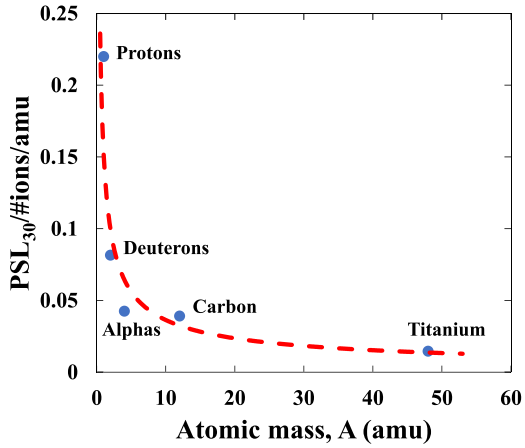

FIG. 8. IP response vs atomic mass unit A for the maximum energy deposited. The maximum energy deposited, represented by the blue points, directly corresponds to the maximum PSL signal, as represented by the response function peaks in Fig. 7. This peak occurs for each ion when the Bragg peak depth is equivalent to the thickness of the active layer.[3,5,6,9] According to SRIM calculations, energetic titanium ions reach this depth in the active layer when they reach 161 MeV. The data are best fitted by a power law (dashed line) $PSL_{30}/ion/amu = 0.1531A^{-0.6244}$.

incident ion energy increases. Figure 7 illustrates this effect in comparing the IP response curves of protons,[5] deuterons,[9] alpha particles,[6] carbon,[3] and titanium. The IP response curve for titanium is plotted in its full range of validity as determined by the deposition length simulations executed in SRIM.

All IP-calibrated ion species have a value corresponding to the peak energy deposited in the IP.[3,5,6,9] There is a general trend of the peak PSL/ion/amu value decreasing with increasing atomic mass units A. Using the peak value from previous calibrations (visualized in Fig. 7), the distribution of the peak PSL response for low-Z ions fits the power model $PSL_{30}/ion/amu = aE^b$. This relationship is strengthened with the inclusion of the PSL_{30}/ion/amu value that corresponds to 161 MeV titanium, as shown in Table II. This latter relationship, plotted in Fig. 8, indicates that the titanium calibration presented in this paper aligns strongly with this power law decay trend.

V. CONCLUSION

The BAS-TR IP has been absolutely calibrated to energetic titanium ions using three charge states, spanning in energy from 6 to 27 MeV. The IP response is independent of charge states and depends solely on the amount of energy deposited within the IP. An empirical power law fit, valid from 4.8 to 161 MeV, can convert the PSL_{30} signal to the absolute number of titanium ions. The uncertainty in PSL for the fitted response function is small, at only ~7%. This calibration provides quantitative measurements of ion energy spectra, allowing for further study in the laser-acceleration of mid-Z ion beams.

Established low-Z calibrations, coupled with the results in this paper, correspond to a power fit law for the peak PSL signal vs atomic mass. From raw IP spectra, absolute spectra of various ions can be roughly approximated, within a factor of 2, using this function. Additional IP calibrations, especially with mid-Z or high-Z ions, would strengthen this empirical relationship. This power law also indicates a decreased sensitivity per nucleon with increasing atomic mass, in agreement with Bonnet's IP model applied to titanium ions. In turn, high-Z ions are predicted to exhibit similar IP response functions.

ACKNOWLEDGMENTS

This material is based on work supported by the Air Force Office of Scientific Research (AFOSR) under Award No. FA9550-14-1-0282 and by the Department of Energy, National Nuclear Security Administration (NNSA) under Award No. DE-NA0003842. The authors also acknowledge the support from the technical staff of the Texas Petawatt Laser at the University of Texas, Austin.

REFERENCES

[1]K. A. Tanaka, T. Yabuuchi, T. Sato, R. Kodama, Y. Kitagawa, T. Takahashi, T. Ikeda, Y. Honda, and S. Okuda, Rev. Sci. Instrum. **76**, 013507 (2005).
[2]J. Miyahara, K. Takahashi, Y. Amemiya, N. Kamiya, and Y. Satow, Nucl. Instrum. Methods Phys. Res., Sect. A **246**, 572 (1986).
[3]D. Doria, S. Kar, H. Ahmed, A. Alejo, J. Fernandez, M. Cerchez, R. Gray, F. Hanton, D. MacLellan, P. McKenna *et al.*, Rev. Sci. Instrum. **86**, 123302 (2015).
[4]B. Maddox, H. Park, B. Remington, N. Izumi, S. Chen, C. Chen, G. Kimminau, Z. Ali, M. Haugh, and Q. Ma, Rev. Sci. Instrum. **82**, 023111 (2011).
[5]A. Mančić, J. Fuchs, P. Antici, S. Gaillard, and P. Audebert, Rev. Sci. Instrum. **79**, 073301 (2008).
[6]T. Bonnet, M. Comet, D. Denis-Petit, F. Gobet, F. Hannachi, M. Tarisien, M. Versteegen, and M. Aléonard, Rev. Sci. Instrum. **84**, 103510 (2013).
[7]T. Bonnet, M. Comet, D. Denis-Petit, F. Gobet, F. Hannachi, M. Tarisien, M. Versteegen, and M. Aleonard, Rev. Sci. Instrum. **84**, 013508 (2013).
[8]N. Rabhi, D. Batani, G. Boutoux, J.-E. Ducret, K. Jakubowska, I. Lantuejoul-Thfoin, C. Nauraye, A. Patriarca, A. Saïd, A. Semsoum *et al.*, Rev. Sci. Instrum. **88**, 113301 (2017).
[9]A. Alejo, S. Kar, H. Ahmed, A. Krygier, D. Doria, R. Clarke, J. Fernandez, R. Freeman, J. Fuchs, A. Green *et al.*, Rev. Sci. Instrum. **85**, 093303 (2014).
[10]C. Freeman, G. Fiksel, C. Stoeckl, N. Sinenian, M. Canfield, G. Graeper, A. Lombardo, C. Stillman, S. Padalino, C. Mileham *et al.*, Rev. Sci. Instrum. **82**, 073301 (2011).
[11]C. Huntington, J. McNaney, E. Gumbrell, A. Krygier, C. Wehrenberg, and H.-S. Park, Rev. Sci. Instrum. **89**, 10G121 (2018).
[12]S. Wilks, A. Langdon, T. Cowan, M. Roth, M. Singh, S. Hatchett, M. Key, D. Pennington, A. MacKinnon, and R. Snavely, Phys. Plasmas **8**, 542 (2001).
[13]A. Robinson, M. Zepf, S. Kar, R. Evans, and C. Bellei, New J. Phys. **10**, 013021 (2008).
[14]L. Yin, B. Albright, B. Hegelich, K. J. Bowers, K. Flippo, T. Kwan, and J. Fernández, Phys. Plasmas **14**, 056706 (2007).
[15]S. Bandyopadhyay, D. Neely, G. Gregori, D. Carroll, P. McKenna, M. Borghesi, F. Lindau, O. Lundh, C. Wahlström, and A. Higginbotham, "Analysis on a wedge-shaped thomson spectrometer for ion studies," Technical Report 1, Central Laser Facility, CCLRC Rutherford Appleton Lab, 2005.

[16]N. Sinenian, M. Rosenberg, M. Manuel, S. McDuffee, D. Casey, A. Zylstra, H. Rinderknecht, M. Gatu Johnson, F. Séguin, J. Frenje *et al.*, Rev. Sci. Instrum. **82**, 103303 (2011).
[17]J. F. Ziegler, M. D. Ziegler, and J. P. Biersack, *SRIM: The Stopping and Range of Ions in Matter* (Cadence Design Systems, 2008).
[18]B. Hidding, G. Pretzler, M. Clever, F. Brandl, F. Zamponi, A. Lübcke, T. Kämpfer, I. Uschmann, E. Förster, U. Schramm *et al.*, Rev. Sci. Instrum. **78**, 083301 (2007).
[19]H. Bethe, Ann. Phys. **397**, 325 (1930).
[20]J. B. Birks, Proc. Phys. Soc., Sect. A **64**, 874 (1951).